The ISME Journal (2015) 9, 1456–1466
© 2015 International Society for Microbial Ecology All rights reserved 1751-7362/15
www.nature.com/ismej

ORIGINAL ARTICLE

Aerobic and anaerobic nitrogen transformation processes in N_2-fixing cyanobacterial aggregates

Isabell Klawonn[1], Stefano Bonaglia[2], Volker Brüchert[2] and Helle Ploug[1,3]
[1]*Stockholm University, Department of Ecology, Environment and Plant Sciences, Stockholm, Sweden;* [2]*Stockholm University, Department of Geological Sciences and Bolin Centre for Climate Research, Stockholm, Sweden and* [3]*University of Gothenburg, Department of Biology and Environmental Sciences, Gothenburg, Sweden*

Colonies of N_2-fixing cyanobacteria are key players in supplying new nitrogen to the ocean, but the biological fate of this fixed nitrogen remains poorly constrained. Here, we report on aerobic and anaerobic microbial nitrogen transformation processes that co-occur within millimetre-sized cyanobacterial aggregates (*Nodularia spumigena*) collected in aerated surface waters in the Baltic Sea. Microelectrode profiles showed steep oxygen gradients inside the aggregates and the potential for nitrous oxide production in the aggregates' anoxic centres. ^{15}N-isotope labelling experiments and nutrient analyses revealed that N_2 fixation, ammonification, nitrification, nitrate reduction to ammonium, denitrification and possibly anaerobic ammonium oxidation (anammox) can co-occur within these consortia. Thus, *N. spumigena* aggregates are potential sites of nitrogen gain, recycling and loss. Rates of nitrate reduction to ammonium and N_2 were limited by low internal nitrification rates and low concentrations of nitrate in the ambient water. Presumably, patterns of N-transformation processes similar to those observed in this study arise also in other phytoplankton colonies, marine snow and fecal pellets. Anoxic microniches, as a pre-condition for anaerobic nitrogen transformations, may occur within large aggregates ($\geqslant$1 mm) even when suspended in fully oxygenated waters, whereas anoxia in small aggregates ($<$1 to $\geqslant$0.1 mm) may only arise in low-oxygenated waters ($\leqslant$25 μM). We propose that the net effect of aggregates on nitrogen loss is negligible in NO_3^--depleted, fully oxygenated (surface) waters. In NO_3^--enriched ($>$1.5 μM), O_2-depleted water layers, for example, in the chemocline of the Baltic Sea or the oceanic mesopelagic zone, aggregates may promote N-recycling and -loss processes.
The ISME Journal (2015) **9,** 1456–1466; doi:10.1038/ismej.2014.232; published online 9 January 2015

Introduction

Aggregates formed by diatoms, cyanobacteria, detritus or fecal pellets are a ubiquitous phenomenon in aquatic environments and of paramount importance for the large-scale energy and nutrient transport through aquatic systems (Alldredge and Silver, 1988; Simon *et al.*, 2002; Paerl and Kuparinen, 2003). At a small scale, phytoplankton colonies and aggregates are highly productive microenvironments characterized by elevated concentrations of organic matter and nutrients. Microorganisms attached to these nutrient oases use the substrate as a food source, for gene exchange, or as refugia from grazers (Grossart and Tang, 2010). During the last two decades, our understanding of aggregate formation, microbial colonization, degradation of organic matter and their overall role in the vertical carbon flux has improved substantially. Lagging far behind is our understanding of microbial nitrogen (N) transformations in aggregates. Hot spots of aerobic and anaerobic microbial N-cycling occur at oxic–anoxic interfaces, such as chemoclines in the water column or at sediment surfaces (Lavik *et al.*, 2009; Stief *et al.*, 2010; Dalsgaard *et al.*, 2013). These zones are characterized by steep oxygen (O_2) gradients resulting in redox-driven niche partitioning of microbial metabolisms (Wright *et al.*, 2012). Such steep physical–chemical gradients also occur in aggregates, but can change abruptly on a micrometre scale and over a short time. For instance, within cyanobacterial aggregates the pH can drop from 9.0 to 7.4 within a few minutes during a light–dark shift, for example, as a cloud passes the sun (Ploug, 2008). Further, O_2 can decline gradually from 100% to $\geqslant$0% air-saturation over a distance of less than one millimetre from the surrounding water into the centre of cyanobacterial colonies, large zooplankton fecal pellets and detritus aggregates (Alldredge and Cohen, 1987; Ploug *et al.*, 1997; Ploug, 2008).

In artificially grown single granules of wastewater treatment reactors, the co-occurrence of nitrification

Correspondence: I Klawonn, Department of Ecology, Environment and Plant Sciences, Stockholm University, SE-106 91 Stockholm, Sweden.
E-mail: isabell.klawonn@su.se
Received 27 May 2014; revised 31 August 2014; accepted 20 October 2014; published online 9 January 2015

and anaerobic ammonium oxidation (anammox) activity has already been demonstrated (Van Hulle *et al.*, 2010). In naturally formed consortia, microorganisms that are active in the anaerobic part of the N-cycle as well as key genes for nitrification and denitrification have been detected for cyanobacterial aggregates (Tuomainen *et al.*, 2003, 2006), but so far only low denitrification activity could be demonstrated in these consortia (Hietanen *et al.*, 2002; Tuomainen *et al.*, 2003).

Here, we examined the physical, chemical and biological constraints for aerobic and anaerobic N-transformation processes within aggregates of the cyanobacteria *Nodularia spumigena* Mertens *ex* Bornet & Flahault, which are common traits of harmful algae blooms in the Baltic Sea (Finni *et al.*, 2001). On the basis of microsensors measurements for high-resolution profiling of dissolved O_2 and nitrous oxide (N_2O), ^{15}N-isotope incubations and sensitive fluorometry analyses, we demonstrate that millimetre-sized aggregates of *N. spumigena* suspended in fully aerated surface waters can host aerobic and anaerobic microbial N-transformations.

Materials and methods

Sampling site and sampling

Single aggregates of *N. spumigena* were collected in a coastal area (58°48′45.48″N; 17°38′47.02″E, 0.1–0.3 nautical miles from the shore, water depth 5 m–20 m) of the Baltic Sea in August 2012. After a few days of calm, sunny weather, aggregates accumulated at the water surface because of their positive buoyancy. The structure of aggregates was compact probably because of enhanced shear forces acting on aggregate formation in coastal areas/archipelagos compared with the open sea. Therefore, aggregates could be sampled directly from the water surface with a bucket. Water disturbance was minimized to preserve the aggregate structure, and single aggregates were selected using the wider end of a glass Pasteur pipette. Water temperature was 18.5 °C and salinity 6.8. A pilot study was conducted in August 2011 at similar environmental conditions.

Characteristics of aggregates and dissolved inorganic N (DIN) in the bulk water

The diameter of each aggregate was first determined with a dissection microscope with an ocular micrometre-scale. Non-spherical aggregates were measured in three dimensions to calculate the equivalent spherical diameter. The surface area and volume was calculated as for a sphere. For analyses of dry weight, particulate organic carbon (POC) and PON, single aggregates ($n = 50$) were collected on pre-weighed, combusted GF/F filters (25 mm, Whatman, Little Chalfont, UK) and frozen at −80 °C. GF/F filters were freeze-dried, decalcified over fuming HCl and analysed for POC and PON using an elemental analyser interfaced to a continuous flow isotope-ratio mass spectrometer (elemental analysis-isotope ratio mass spectrometry; UC Davis Stable Isotope Facility, Davis, CA, USA).

Surface water from the sampling station was taken for analysis of *in situ* concentrations of DIN (NO_3^-, NO_2^-, NH_4^+). Nutrients were determined spectrophotometrically on a segmented flow nutrient analyser system (ALPKEM Flow Solution IV Auto-Analyser, OI Analytical, College Station, TX, USA).

Oxygen and nitrous oxide fluxes

Individual aggregates were fixed in a temperature-controlled (18 °C), vertical flow-through chamber (Ploug and Jørgensen, 1999). An upward flow was set to 0.7 mm s^{-1} and all measurements were conducted in darkness. The O_2 and N_2O microelectrodes were attached to a micromanipulator, and gas concentrations were measured at a vertical resolution $\geqslant$100 μm from the ambient water towards the aggregate's interior (Revsbech, 1989; Andersen *et al.*, 2001). We used a Clark-type O_2 microelectrode (tip diameter <10 μm, 90% response time <1 s, stirring sensitivity <1%; Unisense A/S, Aarhus, Denmark), and a Clark-type N_2O microsensor (tip diameter = 25 μm, response time <15 s, stirring sensitivity <2%; Unisense A/S). The O_2 sensor was calibrated in O_2 air-saturated and in anoxic water prepared by bubbling with N_2 gas. The N_2O sensor calibration was carried out in N_2O-free water and in N_2O-amended water which was prepared by adding a defined aliquot of N_2O-saturated water to a defined volume of water. Oxygen fluxes and rates of O_2-dark respiration of *N. spumigena* were determined mainly in August 2011. The O_2 gradients were measured in two dimensions along the central plane of aggregates suspended in 100% and 30% O_2 air-saturated seawater. In the ambient water, the O_2 concentration was lowered by bubbling with N_2. In August 2012, we conducted a combination of O_2 and N_2O profiling. The N_2O profiling was carried out on aggregates >4 mm kept in (i) *in situ* seawater, (ii) *in situ* seawater + acetylene and (iii) *in situ* seawater + acetylene + NO_3^-. Acetylene (C_2H_2) was added by replacing 5% of the total water volume with C_2H_2-saturated seawater to inhibit the reduction of N_2O to N_2 and thus to induce an accumulation of N_2O when denitrification is present (Yoshinari and Knowles, 1976). In detail, acetylene inhibits the enzyme nitrous oxide reductase in the final step of denitrification and additionally blocks nitrification by inhibiting ammonium monooxygenase in NH_4^+-oxidizing bacteria and archaea. Nitrate was added to a final concentration of 30 μM to overcome diffusion-limited transport of NO_3^- from the ambient water into the centre of the aggregate. Fluxes of O_2 and N_2O, and O_2-respiration rates were calculated using Fick's 1st law (Ploug *et al.*, 1997).

A diffusion coefficient of 1.96×10^{-5} cm^2 s^{-1} for O_2 and 1.97×10^{-5} cm^2 s^{-1} for N_2O at 18 °C was used.

Ammonium release

Aggregates ($n = 10$) were incubated individually in 15 ml Falcon tubes filled with 0.2-μm filtered seawater from the sampling site for 9 h at *in situ* temperature and in darkness. These aggregates were sampled in an enclosed bay close to the initial sampling station where they had been floating for 2 days after newly formed aggregates were sampled (used for O_2/N_2O micro-profiling and ^{15}N-incubations). NH_4^+ concentrations were measured on a fluorometer (Turner Designs, TD-700, Sunnyvale, CA, USA) following the method described by Holmes *et al.* (1999). The NH_4^+ concentration at the start of incubations was 0.52 ± 0.04 μmol l^{-1} ($n = 10$). Ammonification was calculated as total NH_4^+ release minus NH_4^+ derived from N_2 fixation (see below).

The distribution of NH_4^+ inside and around aggregates was modelled using a diffusion-reaction model accounting for the average NH_4^+ production rate per aggregate measured by fluorometry, aggregate size, diffusivity and boundary layer thickness known from the O_2 microprofiles (Ploug *et al.*, 1997). An effective diffusion coefficient of NH_4^+ of 1.60×10^{-5} cm^2 s^{-1} was used inside the aggregates (Li and Gregory, 1974).

^{15}N incubations: N_2 fixation/NH_4^+ release, nitrification, NO_3^- reduction to ammonium, denitrification and anammox

N. spumigena aggregates, which were sampled together with the ones used for analyses of O_2 and N_2O fluxes, were incubated individually for 9 and 14 h in a 5.9 ml Exetainer vial (Labco, Lampeter, UK) in darkness at *in situ* temperature (18 °C). Each vial was filled with 0.2-μm-filtered aerated seawater from the sampling site. The Exetainer vials were rotated during the incubations assuring that aggregates were free-floating to support the diffusion of solutes into the aggregates (Ploug and Grossart, 1999).

The ^{15}N isotope pairing technique was applied to target processes of the N-cycle (Nielsen, 1992; Thamdrup and Dalsgaard, 2002), while different combinations of labelled and non-labelled N-compounds were used (incubations I–VII, Table 1). The substrates $^{15}NO_3^-$, $^{15}NH_4^+$ and $^{14}NO_3^-$, $^{14}NO_2^-$, $^{14}NH_4^+$ were added to a final concentration of 30.0 ± 1.3 μM (mean ± s.d., $n = 14$).

One treatment (incubation II) was used to quantify N_2 fixation and to track the release of NH_4^+ during N_2 fixation. $^{15}N_2$ was added as an aliquot of $^{15}N_2$-amended water, which was prepared prior incubations by enriching 0.2 μm-filtered sea water from the sampling station with $^{15}N_2$ gas (Mohr *et al.*, 2010). The final $^{15}N_2$ label was 1.8 ± 0.1 atom% ($n = 5$), as determined by gas chromatographic isotope ratio mass spectrometry. Aggregates were filtered on GF/F filters (25 mm, Whatman), and the incorporation of $^{15}N_2$ gas via N_2 fixation into biomass was analysed by elemental analysis-isotope ratio mass spectrometry (UC Davis Stable Isotope Facility). Rates of N_2 fixation were calculated from the measured ^{15}N atom% excess in the water and particulate N on the filter, and related to the total N_2 gas in the water and particulate nitrogen per aggregates (Montoya *et al.*, 1996). The filtrate was stored in an Exetainer vial for analysis of the released $^{15}NH_4^+$ via mass spectrometry.

Table 1 Design of incubations with ^{15}N-labelled N-compounds to distinguish N-pathways within individual *N. spumigena* aggregates

ID	*Isotope addition*	*Targeted process*	*Targeted product*
I	No label	Control	$^{15}NO_3^-$, $^{15}NO_2^-$, $^{15}NH_4^+$
II	$^{15}N_2$	N_2 fixation	PO^{15}N[a], $^{15}NH_4^+$
III	$^{15}NH_4^+$	Nitrification	$^{15}NO_3^-$, $^{15}NO_2^-$
IV	$^{15}NO_3/^{14}NH_4^+$	NO_3^- reduction to NH_4^+	$^{15}NH_4^+$
		Denitrification	N_2 (^{15}N ^{15}N)
V	$^{15}NO_3^-$	NO_3^- reduction to NH_4^+	$^{15}NH_4^+$
		Denitrification	N_2 (^{15}N ^{15}N)
VI	$^{15}NO_3^-/^{14}NO_3^-$	Denitrification	N_2 (^{15}N ^{15}N), (^{15}N ^{14}N)
VII	$^{15}NH_4^+/^{14}NO_2^-$	Anammox[b]	N_2 (^{15}N ^{14}N)

[a]PO^{15}N—Particulate organic ^{15}N-nitrogen.
[b]Anammox—anaerobic ammonium oxidation.

The isotope ratios of $^{28}N_2$, $^{29}N_2$ and $^{30}N_2$ were analysed by gas chromatographic isotope ratio mass spectrometry on a Thermo Delta V isotope ratio mass spectrometer (IGV SIL, Stockholm University, Stockholm, Sweden). Controls without label were used to determine the background isotopic composition of N_2, NH_4^+ and NO_3^-/NO_2^-. The N-isotope composition of NH_4^+ was analysed after chemical conversion of NH_4^+ to N_2 with alkaline hypobromite (NaOBr) (Warembourg, 1993). The N-isotope composition of NO_3^- and NO_2^- was validated after reduction of NO_3^- to NO_2^- with cadmium and conversion of NO_2^- to N_2 using sulphamic acid (Füssel *et al.*, 2012).

The production of N_2, NH_4^+ and NO_2^-/NO_3^- was calculated from the excess concentrations of ^{15}N-nitrogen relative to air, and corrected for the fraction of natural abundant ^{15}N in the total substrate pool. Rates in individual aggregates were computed from the concentrations of ^{15}N-compounds produced versus time. Statistically significant production of ^{15}N-labelled products was tested against controls (*t*-test at a confidence interval of 95% for normally distributed variables; Mann–Whitney U-test for non-normal distributed variables).

Nitrate demand

Fluxes of NO_3^- between the ambient water and the aggregate were modelled using the same diffusion-reaction model as for NH_4^+. The NO_3^- concentration

profile and theoretical demand of NO_3^- in the ambient water were calculated for the average measured rates of NO_3^- reduction to N_2O and NH_4^+, respectively. An effective molecular diffusion coefficient of 1.53×10^{-5} cm^2 s^{-1} at 18 °C was used in the flux calculations (Li and Gregory, 1974).

Results

Characteristics of aggregates and DIN in the natural water
Characteristics of *N. spumigena* aggregates sampled in August 2012 are summarized in Table 2. Aggregates were large (⩾3 mm) and compact (Figure 1a). Concentrations of DIN in the *in situ* water were 0.47 ± 0.13 µmol NO_3^- l^{-1} (mean ± s.d., $n = 12$), 0.05 ± 0.01 µmol NO_2^- l^{-1} ($n = 12$) and 0.27 ± 0.06 µmol NH_4^+ l^{-1} ($n = 11$).

Table 2 Characteristics of single *N. spumigena* aggregates used for stable isotope incubations and microsensor analyses

	Mean ± s.d.	*Min*	*Max*
Dry weight (mg)	1.6 ± 0.5 ($n = 50$)	0.4	3.2
Diameter (mm)	4.7 ± 0.9 ($n = 150$)	3.0	7.0
Surface area (cm^2)	0.7 ± 0.3 ($n = 150$)	0.3	1.5
Volume (cm^3)	0.06 ± 0.03 ($n = 150$)	0.01	0.18
POC (µg)	287 ± 106 ($n = 50$)	138	586
POC (% of DW)	19 ± 6 ($n = 50$)	10	39
PON (µg)	53 ± 20 ($n = 50$)	23	110
C:N ratio	5.4 ± 0.4 ($n = 50$)	4.4	6.0

Abbreviations: DW, dry weight; POC, particulate organic carbon; PON, particulate organic nitrogen
The number of aggregates that have been examined is given as *n*.

Oxygen and nitrous oxide fluxes
Dark respiration ranged between 33 and 94 nmol O_2 agg^{-1} h^{-1} for individual aggregates with equivalent spherical diameters between 4.9 and 6.7 mm. These respiration rates were similar to those in August 2009 and 2011, when dark respiration varied between 0.038 and 87 nmol O_2 h^{-1} in *Nodularia* colonies with diameters from 0.3 to 5.0 mm (see also Ploug *et al.*, 2011). Many aggregates of *N. spumigena* held interior anoxia because of their size, high respiration rates and their compact structure. The respiratory O_2 consumption was thus limited by diffusion of O_2 from the ambient water into the aggregates (Figure 1b). The size of the anoxic core was dependent on the O_2 concentration in the ambient water, that is, the anoxic interior expanded from 5% of the total aggregate volume as an aggregate was suspended in 100% air-saturated water to >95% in 30% air-saturated water (Figures 1b and c).

No N_2O production was detected when aggregates were kept in (i) seawater or (ii) seawater + C_2H_2. After the addition of NO_3^- (treatment (iii) seawater + C_2H_2 + NO_3^-), an increasing N_2O gradient was recorded from the ambient seawater into the centre of the aggregates, showing that N_2O production was limited by NO_3^- (Figure 2a). The N_2O flux at the aggregate surface was 0.26 nmol N_2O cm^{-2} h^{-1} (= 0.53 nmol N cm^{-2} h^{-1}). In treatment (iii) the N_2O microsensor was not only used to record the N_2O concentration from the ambient water towards the aggregate (see above). This treatment was also used to place the N_2O microsensor in the

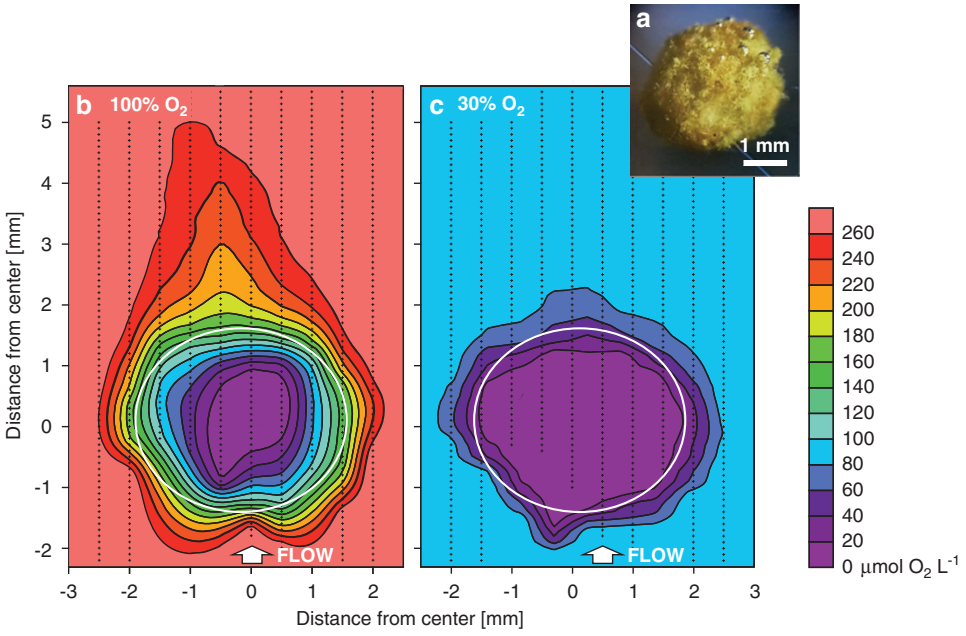

Figure 1 (**a**) Photograph of a *N. spumigena* aggregate. (**b** and **c**) Isopleths of O_2 around and inside a *N. spumigena* aggregate (equivalent spherical diameter = 3.1 mm) in O_2 air-saturated (100%) and low-saturated water (30%) during darkness. Dark respiration (46 nmol O_2 agg^{-1} h^{-1} at 100% O_2, and 28 nmol O_2 agg^{-1} h^{-1} at 30% O_2) created sharp microscale oxyclines. The anoxic interior comprised about 5% of the total aggregate volume in 100% O_2 air-saturated water and expanded to >95% in 30% O_2 air-saturated water. Oxygen was measured with an O_2 microsensor in two dimensions with a high spatial resolution (100 µm × 500 µm; shown as crosses). The flow velocity from below was 0.7 mm s^{-1} (white arrow). The aggregate surface is marked as a white circle.

centre of the aggregate to record the potential N_2O accumulation over time within the aggregates when no advective solute transport took place. As soon as the water flow was stopped, the anoxic core expanded as the O_2 diffusion into the centre decreased. Concurrently, the transport of N_2O away from the aggregate decreased, and the N_2O concentration within the aggregate centre increased at a rate of 1.8–3.6 μM h^{-1} (Figure 2b). The maximum N_2O concentration in the centre of the aggregate was 0.9–2.2 μM. Please note that the latter measurements confirm the potential of N_2O production within the aggregates, but the increase in N_2O concentration in the interior cannot be used to calculate a N_2O flux following Fick's 1st law of diffusion because the microsensor was kept stationary within the aggregate.

Ammonium release

Two sources of NH_4^+ release were investigated: (a) NH_4^+ release derived from N_2 fixation and (b) ammonification. NH_4^+ derived from N_2 fixation was 1.51 ± 1.10 nmol NH_4^+ cm^{-2} h^{-1} ($n = 5$, 9 h incubations, see below), and the total NH_4^+ release was 12.9 ± 5.3 nmol NH_4^+ cm^{-2} h^{-1} ($n = 10$, 9 h incubations). Thus, about 12% of the total NH_4^+ release derived from N_2 fixation and 88% could presumably be attributed to ammonification. The distribution of the NH_4^+ concentration was modelled for the boundary layer at the aggregate–water interface and the interior of colonies. Cyanobacterial aggregates were net sources of NH_4^+ to the ambient water, indicated by the increase in NH_4^+ concentration from 0.52 μM in the ambient water to 35 μM in the centre (Figure 3).

N_2 fixation/NH_4^+ release, nitrification, NO_3^- reduction to NH_4^+, denitrification and anammox

Pathways of N-cycling were measured by the isotope pairing technique for individual *N. spumigena* aggregates in darkness. We detected a net production of ^{15}N compounds in ⩾95% of all ^{15}N-labelled tracer incubations. The means of all sets of ^{15}N incubations, each with $n = 5$–30, were significantly different from controls (*t* test/U test, $P < 0.05$; see Table 3). All reported rates were net rates, that is, minimum estimates because the concentration of a ^{15}N product was most likely diminished by co-occurring assimilation or dissimilation.

Beside ammonification (see above), the highest rates were found for dark N_2 fixation (including concurrent NH_4^+ leakage) and for nitrate reduction to ammonium, up to 1.3 and 1.7 nmol N cm^{-2} h^{-1}, respectively. Of the gross N_2 fixation (N_2 incorporation + NH_4^+ release), 34.8 ± 21.8% ($n = 10$) were released as NH_4^+ to the surrounding water. Mean net rates of NO_3^- production via nitrification ranged between 0.004 and 0.006 nmol N cm^{-2} h^{-1}, and net NO_2^- production via nitrification was below

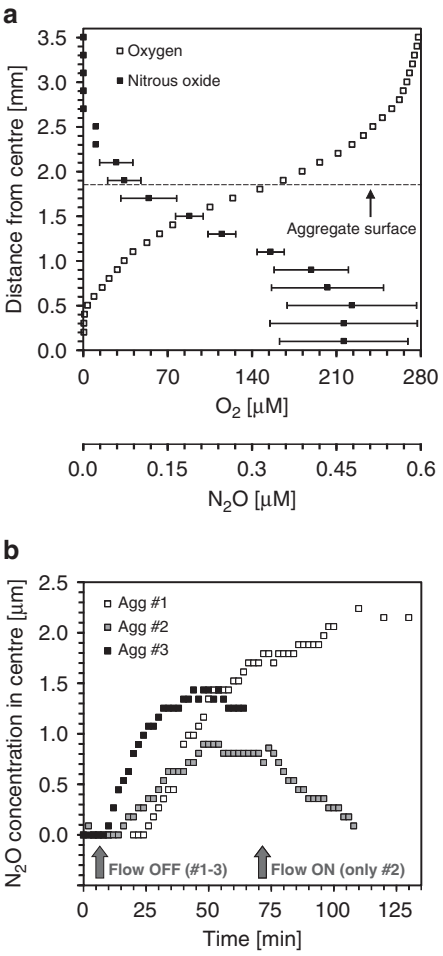

Figure 2 (**a**) Distribution of O_2 and N_2O concentration (mean ± s.d., $n = 3$) within a *N. spumigena* aggregate (equivalent spherical diameter = 4.9 mm) during darkness. Dark respiration (126 nmol O_2 cm^{-2} h^{-1}) led to O_2 depletion in the aggregate centre, where nitrous oxide was produced and transported outwards via diffusion. The N_2O flux at the aggregates' surface was 0.26 nmol N_2O cm^{-2} h^{-1}, and the ratio of O_2 consumption to N_2O release flux was 480:1. The flow velocity from below the aggregate was 0.7 mm s^{-1}. (**b**) N_2O accumulation in the centre of *N. spumigena* aggregates during darkness. A N_2O microsensor was placed in the aggregate's centre and N_2O production was recorded over time. At time zero, the upward flow of 0.7 mm s^{-1} was switched off (grey arrow on the left). For aggregate #2 the flow was re-started after 70 min (grey arrow on the right) showing that advective solute transport at the aggregate–water interface was enhanced because of the water flow, which restricted N_2O accumulation in the aggregate centre. (**a** and **b**) All N_2O measurements were conducted in seawater enriched with C_2H_2-saturated seawater (5%) and NO_3^- (30 μM). No N_2O production was detected before adding C_2H_2 and NO_3^-.

the detection limit. The mean N_2 production rates of 0.008–0.037 nmol N cm^{-2} h^{-1} due to denitrification were lower than the rates of N_2O production in the presence of C_2H_2 indicating an incomplete reduction of NO_3^- to N_2 (please see discussion). Of all anaerobic microbial N conversion rates, anammox rates were consistently the lowest. In the experiments conducted in 2011, the $^{29}N_2$ signal from $^{15}NH_4^+/^{14}NO_2^-$ incubations was slightly higher than in the 2012 experiments, up to 0.042 nmol N cm^{-2} h^{-1} ($n = 32$), but it

cannot be excluded that the $^{29}N_2$ signal produced in these incubations at least partly originated from coupled nitrification–denitrification instead of anammox. An overview of microbial N-transformation processes and their relative importance after 9 h incubations is given in Figure 4.

Potential nitrate demand

The modelled NO_3^- concentration profile showed that a NO_3^- concentration $\geqslant 1.5\,\mu M$ in the ambient water was required to supply sufficient NO_3^- for the measured N_2O flux (0.26 nmol $N_2O\,cm^{-2}\,h^{-1}$, Figure 2a) under C_2H_2 inhibition. To balance the formation of N_2O and NH_4^+ by NO_3^- reduction 0.26 nmol $N_2O\ cm^{-2}\ h^{-1}$ plus 1.7 nmol $NH_4^+\ cm^{-2}\ h^{-1}$, an ambient concentration of 6.3 µmol $NO_3^-\ l^{-1}$ was required. This indicates that under the experimental conditions of 30 µmol $NO_3^-\ l^{-1}$, the mean NO_3^- reduction rate was not limited by NO_3^- diffusion from the ambient water into the aggregate (Figure 5). Under natural conditions, however, nitrate reduction to N_2O/N_2 or NH_4^+ was likely limited by low internal nitrification activity and low NO_3^- concentrations in the ambient water ($<1\,\mu M$).

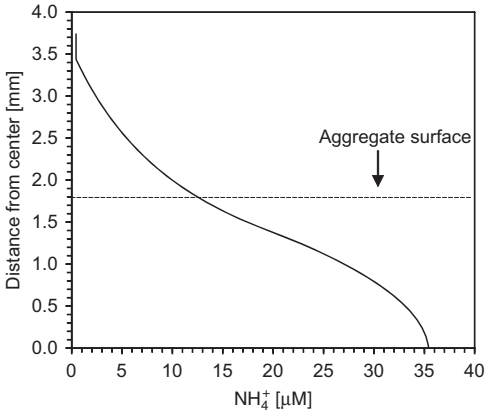

Figure 3 Modelled distribution of NH_4^+ in the boundary layer and inside a *N. spumigena* aggregate. Owing to steep gradients of the solute from the aggregates' interior towards the ambient water, colonies were net sources of NH_4^+ with high NH_4^+ fluxes of 12.9 nmol $cm^{-2}\ h^{-1}$ off the aggregates' surfaces.

Discussion

Microbial N-transformations in N. spumigena aggregates—who is dominating and why?

Phytoplankton colonies and aggregates often have relatively short lifetimes and seldom provide a temporally and spatially stable environment. Nonetheless, this study showed that physical, chemical and biological constraints within these aggregates can act in concert to produce a dynamic, millimetre-sized consortium with co-existing aerobic and anaerobic N-transformations.

Dark N_2 fixation rates and the surplus of NH_4^+ in the water which derived from N_2 fixation were higher after 9 h incubations than after 14 h incubations. Part of the fixed N might have been transferred to bacteria, which detached from the aggregate (Kiørboe *et al.*, 2002). Moreover, after prolonged darkness, N_2 fixation in *N. spumigena* was likely limited by depleted intracellular energy resources.

Table 3 Potential rates of nitrogen transformations for *N. spumigena* aggregates after 9 and 14 h incubations in darkness

	Incubation time	*Rate (mean ± s.d.) per aggregate*	*Rate (mean ± s.d.) per surface area*
N_2 fixation		*nmol N agg^{-1} h^{-1}*	*nmol N cm^{-2} h^{-1}*
	9 h	0.67 ± 0.27*	1.3 ± 0.8 ($n=10$)
	14 h	0.45 ± 0.32*	0.7 ± 0.5 ($n=10$)
NH_4^+ release (from N_2 fixation)		*nmol NH_4^+ agg^{-1} h^{-1}*	*nmol NH_4^+ cm^{-2} h^{-1}*
	9 h	0.65 ± 0.29*	1.51 ± 1.10 ($n=5$)
	14 h	0.05 ± 0.05*	0.07 ± 0.06 ($n=5$)
Total NH_4^+ release		*nmol NH_4^+ agg^{-1} h^{-1}*	*nmol NH_4^+ cm^{-2} h^{-1}*
	9 h	7.5 ± 3.0*	12.9 ± 5.3 ($n=10$)
Nitrification		*nmol NO_3^- agg^{-1} h^{-1}*	*nmol NO_3^- cm^{-2} h^{-1}*
	9 h	0.004 ± 0.004*	0.006 ± 0.006 ($n=10$)
	14 h	0.002 ± 0.002*	0.004 ± 0.007 ($n=10$)
NO_3^- reduction to NH_4^+		*nmol NH_4^+ agg^{-1} h^{-1}*	*nmol NH_4^+ cm^{-2} h^{-1}*
	9 h	1.1 ± 1.1*	1.7 ± 1.6 ($n=20$)
	14 h	1.1 ± 0.9*	1.2 ± 0.7 ($n=19$)
Denitrification		*nmol N agg^{-} h^{-1}*	*nmol N cm^{-2} h^{-1}*
	9 h	0.008 ± 0.007*	0.013 ± 0.008 ($n=30$)
	14 h	0.031 ± 0.024*	0.037 ± 0.024 ($n=29$)
Anammox		*nmol N agg^{-1} h^{-1}*	*nmol N cm^{-2} h^{-1}*
	9 h	0.000 ± 0.001*	0.001 ± 0.001 ($n=20$)
	14 h	0.001 ± 0.000*	0.001 ± 0.001 ($n=19$)

Rates are given per aggregate and per surface area. The number of aggregates that have been incubated individually is given as *n*. Statistical significance was tested against controls.
*$P<0.05$.

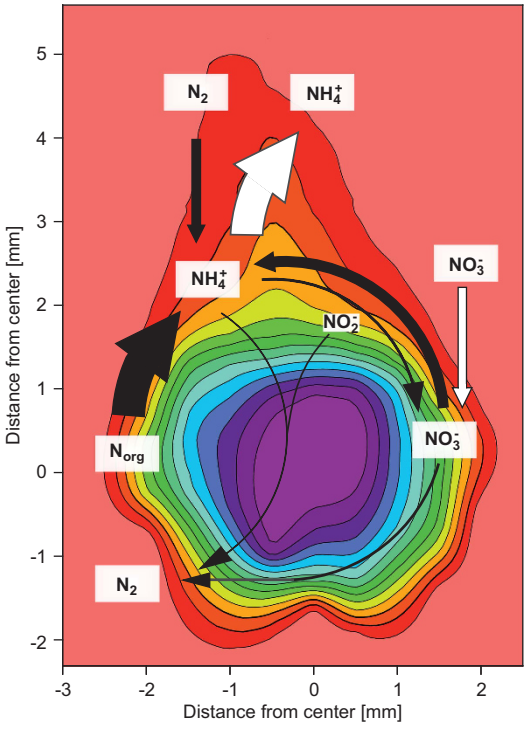

Figure 4 Schematic overview of potential nitrogen transformation processes in *N. spumigena* aggregates. N_2 fixation and ammonification supplied sufficient amounts of NH_4^+. This could have been oxidized to fuel the demand of NO_3^- reduction, but nitrification rates limited the internal N-recycling and -loss processes. The width of arrows outlines the relative importance of net rates measured under conditions of substrate availability after 9 h incubations (compare with Table 3). N_2 fixation/NH_4^+ release and ammonification were determined in non-enriched experiments. For nitrification, nitrate reduction to N_2/NH_4^+ and anammox, the substrate was added to the water (30 μM). The white arrows indicate *N. spumigena* aggregates as net NH_4^+ sources and net NO_3^- sinks.

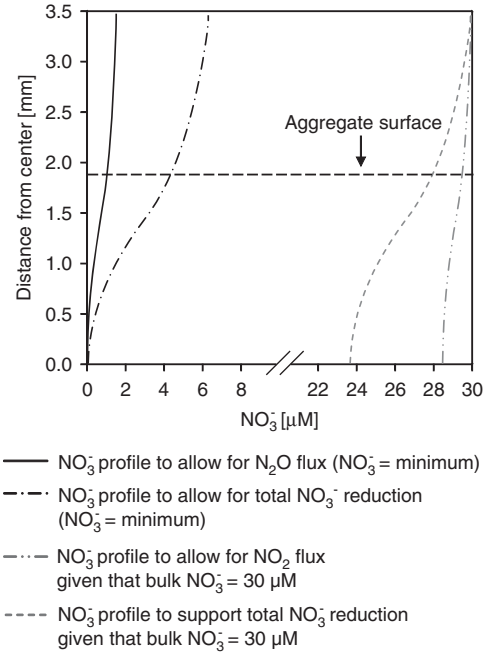

Figure 5 Modelled distribution of NO_3^- in the boundary layer and inside a *N. spumigena* aggregate based on measured O_2 and N_2O profiles (Figure 2a). A minimum NO_3^- concentration in the ambient water of 1.5 and 6.3 μM is required to support the N_2O flux of 0.26 nmol cm^{-2} h^{-1} (see Figure 2a) and the total NO_3^- reduction rate (0.26 nmol N_2O cm^{-2} h^{-1} plus 1.7 nmol NH_4^+ cm^{-2} h^{-1}, see also Table 3) at the surface of individual aggregates, respectively. During incubations of *N. spumigena* aggregates, the ambient NO_3^- concentrations were high with 30 μM to prevent NO_3^--diffusion limitation.

Heterotrophic N_2 fixation has been reported in aphotic, deep waters of the Baltic Sea (Farnelid *et al.*, 2009, 2013) and elsewhere (Rahav *et al.*, 2013), but we assume that N_2 fixation in *N. spumigena* aggregates ceases when they are exposed to prolonged darkness, and ammonification remains as the sole NH_4^+ source.

A large fraction of the NH_4^+ was lost to the surrounding water because of the steep concentration gradients (Figure 3), or served as an internal source of DIN for other members of the microbial community in the aggregate. Of those, anammox bacteria were of least importance. Compared with chemical gradients in chemoclines or in sediments where anammox can contribute significantly to N-losses (Lam and Kuypers, 2011), the physicochemical gradients in aggregates are far more unstable (Ploug *et al.*, 1997). Thus, the growth of anammox bacteria with doubling times of several days might be restricted in aggregates (Strous *et al.*, 1999). Nitrifying bacteria and archaea can have shorter doubling times of 1–2 days (Ward *et al.*, 2007), and the presence of nitrifiers (likely *Nitrospira*) as well as key genes for nitrification and denitrification (*amoA, nirS, nirK*) have been demonstrated in *N. spumigena* aggregates (Tuomainen *et al.*, 2003, 2006). In our study, net nitrification was low despite high concentrations of internal NH_4^+ and ambient O_2, but the actual nitrifying activity was masked by the removal of $^{15}NO_3^-$ because of high rates of NO_3^- reduction. After incubations with $^{15}NH_4^+$/$^{14}NO_2^-$, 70 ± 17% ($n = 20$) of the ^{15}N-N_2 was detected as $^{15}N^{15}N$, which indicates coupled nitrification–denitrification. Also, incubations with $^{15}NO_3^-$ to target denitrification showed a significant formation of $^{29}N_2$ in excess to the low *in situ* concentrations of $^{14}NO_3^-$. Accordingly, 5.9 ± 2.9% ($n = 19$) of the NO_3^- reduction originated from $^{14}NO_2^-$/$^{14}NO_3^-$ that was not added as a tracer but was oxidized by nitrifiers using the NH_4^+ released from the aggregates. The corresponding gross nitrification rates were as high as 0.09 ± 0.07 nmol NH_4^+ cm^{-2} h^{-1} ($n = 39$)—ca. 20-fold higher than the net rates given in Table 3.

Aggregates of *N. spumigena* responded to NO_3^- exposure by reduction to NH_4^+, which retained inorganic N in the vicinity of the consortia instead of losing it as N_2 by denitrification. It is, however, difficult to separate dissimilatory and assimilatory pathways of ^{15}N-NO_3^- reduction based on our measurements. Strains of *N. spumigena* isolated from the Baltic Sea have a low NO_3^- affinity (Vintila and El-Shehawy, 2010; Kabir and El-Shehawy,

2012), but in our incubations, NO_3^- concentrations were high (30 μM), and thus NO_3^- assimilation by *N. spumigena* cannot be excluded. Moreover, NO_3^- reduction can be explained by the activity of a diverse group of bacteria, protists and eukaryotic algae which are associated with *N. spumigena* aggregates (Salomon *et al.*, 2003; Stoecker *et al.*, 2005; Tuomainen *et al.*, 2006). Therefore, the respective share of dissimilatory and assimilatory pathways in NO_3^- reduction in *N. spumigena* aggregates remains uncertain.

Net N_2 production via denitrification was about two orders of magnitude lower than NO_3^- reduction to NH_4^+. The N_2 production rates detected in the ^{15}N-NO_3^- incubations, however, were more than 10 times lower than the rates of N_2O production in the presence of C_2H_2 indicating that, even without the inhibitor, a large amount of NO_3^- was not reduced to N_2. Possible explanations could be that denitrifiers produced N_2O instead of N_2 under aerobic conditions (Takaya *et al.*, 2003), or that a low pH of 7.4 inside *N. spumigena* aggregates during darkness (Ploug, 2008) led to an incomplete denitrification (Thomsen *et al.*, 1994). Nevertheless, most likely the usage of two different experimental set-ups to measure N_2 and N_2O production—one using ^{15}N-isotope incubations lasting for up to 14 h and the other applying microsensors to record the instantaneous N_2O production inside aggregates after NO_3^- exposure in the presence of C_2H_2—yielded different results. Therefore, solid conclusions on the N_2O:N_2 ratios should await further studies.

In our incubations, the aggregate-attached denitrifying bacteria faced neither strict O_2 nor organic C limitation, but NO_3^- limitation. This is supported by the micromolar-concentrations of N_2O that accumulated inside the anoxic interior (Figure 2) less than 1 h after NO_3^- was added to the N-depleted water—the duration which corresponds to the diffusion time of NO_3^- into the aggregates. Most denitrifying bacteria are facultative anaerobes (Zumft, 1997), that is, attached denitrifying bacteria may switch from O_2 respiration to NO_3^- respiration at persistent low O_2 and elevated NO_3^- concentrations. This assumption is supported by the observation that 61% of the total ^{15}N-NO_3^- label (30 μM) was recovered as N_2 and 39% as NH_4^+ after one aggregate was left in anoxic water for several weeks. In this case, denitrification activity even exceeded rates of NO_3^- reduction to NH_4^+.

Microbial N-transformations in aggregates suspended in surface waters or in O_2-depleted, NO_3^--enriched subsurface waters

Oxygen depletion inside aggregates is a prerequisite for anaerobic N-transformation. In Figure 6, we compiled O_2-respiration rates measured on aggregates of different sizes and sources from previous studies. For reference, we plotted the modelled respiration rate needed for the aggregates' interiors to turn anoxic: In O_2 air-saturated water ($O_2 = 250$ μM), anoxia occurred within cyanobacterial colonies ⩾1 mm or (diatom) macroaggregates of upwelling zones. For smaller aggregates and zooplankton fecal pellets, the measured respiration rates were 1–2 order of magnitudes lower than the respiration rate required for these to turn anoxic (Figure 6). Accordingly, anaerobic N-recycling and -loss processes present in fully aerated waters seemed to be restricted to large, compact aggregates or colonies formed by, for example, *N. spumigena* or *Trichodesmium* spp. The N_2-fixing cyanobacteria *Trichodesmium* spp. accounts for a gross of the global marine N_2 fixation (Capone *et al.*, 1997; Karl *et al.*, 2002); and similarities between *N. spumigena* and *Trichodesmium* spp. in terms of aggregate formation,

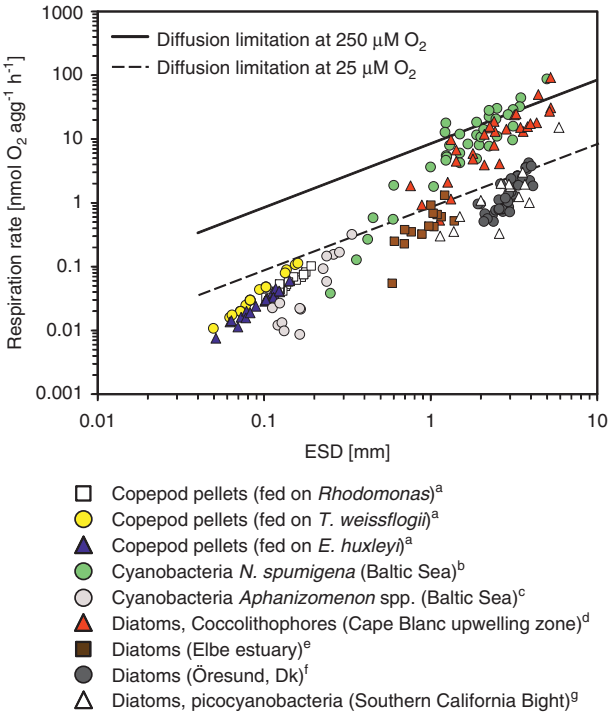

Figure 6 Respiration rates of aggregates of various sources and sizes and their potential of central anoxia. High rates of aerobic respiration can lead to O_2-depletion in the aggregate centre as the diffusion of O_2 from the ambient water inwards the aggregate is insufficient to compensate for the internal O_2 consumption. The reference respiration rate which predicts the aggregates to turn anoxic in their centre when floating in fully oxygenated water (250 μmol O_2 l^{-1}) or in low-oxygen waters (25 μmol O_2 l^{-1}) are shown as a straight and dashed line, respectively. At ambient O_2 concentrations of 250 μM, anoxic conditions may occur within cyanobacterial colonies ⩾1 mm or (diatom) macroaggregates. At 25 μmol O_2 l^{-1}, even smaller phytoplankton aggregates, detritus as well as fecal pellets (<1 mm to ⩾0.1 mm) can become anoxic. The reference respiration rate needed for aggregates or colonies to turn anoxic in their centre at a bulk O_2 concentration of 25 or 250 μM was calculated according to Ploug *et al.* (1997) assuming an apparent diffusivity inside aggregates of 0.9 times the molecular diffusion coefficient in water (Ploug *et al.*, 2008). Data of respiration rates are compiled from previous studies of [a]Ploug *et al.* (2008), [b]Ploug *et al.* (2011), [c]Ploug *et al.* (2010), [d]Iversen and Ploug (2010), [e]Ploug *et al.* (2002), [f]Grossart *et al.* (2003) and [g]Ploug *et al.* (1999).

the development of microscale oxyclines (Paerl and Bebout, 1988), and NH_4^+ remineralisation (Mulholland and Capone, 2000) suggest that a redox-driven niche partitioning of microbial N-transformation processes may not only exist in *N. spumigena* but also in *Trichodesmium* spp. Yet, diazotrophic cyanobacterial colonies accumulate in N-depleted surface waters during bloom periods. We therefore presume that their effect as N-sink is negligible in the oxygenated, NO_3^--depleted photic zone.

As senescing aggregates sink out of the surface layer, they can enter water depths that are NO_3^--enriched, for example, at the Landsort Deep in the Baltic Sea at $\geqslant 30$ m depths ($\geqslant 1.5$ μM NO_3^-, Swedish Environmental Monitoring Program) and in global waters at depths of >200 m (>10 μM NO_3^-) or non-sulphidic O_2 minimum zones (25 μM NO_3^-) (Karl *et al.*, 2003; Kuypers *et al.*, 2005; Johnson *et al.*, 2010). In these zones, NO_3^- concentrations are sufficient to support NO_3^- reduction rates as found in our study (Figure 5). Moreover, these water layers are often accompanied by hypoxia or anoxia. At low ambient O_2, the anoxic core, and thus the site for anaerobic respiration within cyanobacterial aggregates, expanded substantially (Figure 1). Additionally, not only large but also smaller phytoplankton aggregates, detritus and fecal pellets (<1 mm to $\geqslant 0.1$ mm) were predicted to become anoxic (Figure 6). We therefore suggest that anaerobic N-transformations in aphotic O_2-depleted waters are promoted by particulate material (Lam and Kuypers, 2011; Ulloa *et al.*, 2012; Ganesh *et al.*, 2014). Nonetheless, our measurements with aggregates at 18 °C are not directly applicable to the mesopelagic zone where microbial processes in senescent aggregates decrease because of lower temperatures (Iversen and Ploug, 2013). Moreover, the potential of aggregates to significantly contribute to the N-cycling in O_2-deficient, NO_3^--enriched waters might be limited by their short residence times within these zones and the exponential decline of particulate organic material within the first hundred meters water depth (Martin *et al.*, 1987). Hence, in future studies, the particle size distribution within these zones should be investigated in combination with small-scale fluxes of N within settling aggregates allowing for the temporal variation of the microbial community, and the effect of low ambient O_2 availability and low temperature on the activity of aggregate-attached microbes.

Conflict of Interest

The authors declare no conflict of interest.

Acknowledgements

This work was supported by The Swedish Research Council for Environment, Agricultural Sciences and Spatial Planning, FORMAS (Grant no. 215-2009-813 to Ragnar Elmgren, H.P., and V.B. Grant nr. 215-2010-779 to H.P.), by the Baltic Ecosystem Adaptive Management (BEAM to H.P. and to V.B.), and the Baltic Sea Centre, Stockholm University (Askö grant to I.K. and S.B.). We are grateful for the technical advice by Heike Siegmund (SIL-Stable Isotope Laboratory, Stockholm), Hannah Marchant, Jessica Füssel and Gaute Lavik (Max Planck Institute for Marine Microbiology, Bremen, Germany) during GC-IRMS measurements. We would like to thank Silvia Fedrizzi and the staff at the Askö Marine Research Station for their assistance during sampling; and Anders Sjösten and team for nutrient analyses. We are also grateful for the thoughtful comments of three anonymous reviewers.

References

Alldredge AL, Cohen Y. (1987). Can microscale chemical patches persist in the sea? Microelectrode study of marine snow, fecal pellets. *Science* **235**: 689–691.

Alldredge AL, Silver MW. (1988). Characteristics, dynamics and significance of marine snow. *Prog Oceanogr* **20**: 41–82.

Andersen K, Kjar T, Revsbech NP. (2001). An oxygen insensitive microsensor for nitrous oxide. *Sensors and Actuators, B: Chemical* **81**: 42–48.

Capone DG, Zehr JP, Paerl HW, Bergman B, Carpenter EJ. (1997). Trichodesmium, a globally significant marine cyanobacterium. *Science* **276**: 1221–1229.

Dalsgaard T, De Brabandere L, Hall POJ. (2013). Denitrification in the water column of the central Baltic Sea. *Geochim Cosmochim Acta* **106**: 247–260.

Farnelid H, Bentzon-Tilia M, Andersson AF, Bertilsson S, Jost G, Labrenz M *et al.* (2013). Active nitrogen-fixing heterotrophic bacteria at and below the chemocline of the central Baltic Sea. *ISME J* **7**: 1413–1423.

Farnelid H, Öberg T, Riemann L. (2009). Identity and dynamics of putative N_2-fixing picoplankton in the Baltic Sea proper suggest complex patterns of regulation. *Environmental microbiology reports* **1**: 145–154.

Finni T, Kononen K, Olsonen R, Wallström K. (2001). The history of cyanobacterial blooms in the Baltic Sea. *Ambio* **30**: 172–178.

Füssel J, Lam P, Lavik G, Jensen MM, Holtappels M, Günter M *et al.* (2012). Nitrite oxidation in the Namibian oxygen minimum zone. *ISME J* **6**: 1200–1209.

Ganesh S, Parris DJ, Delong EF, Stewart FJ. (2014). Metagenomic analysis of size-fractionated picoplankton in a marine oxygen minimum zone. *ISME J* **8**: 187–211.

Grossart HP, Hietanen S, Ploug H. (2003). Microbial dynamics on diatom aggregates in Øresund, Denmark. *Mar Ecol Prog Ser* **249**: 69–78.

Grossart HP, Tang KW. (2010). Available from www.aquaticmicrobial.net. *Commun Integr Biol* **3**: 491–494.

Hietanen S, Moisander PH, Kuparinen J, Tuominen L. (2002). No sign of denitrification in a Baltic Sea cyanobacterial bloom. *Mar Ecol Prog Ser* **242**: 73–82.

Holmes RM, Aminot A, Kérouel R, Hooker BA, Peterson BJ. (1999). A simple and precise method for measuring ammonium in marine and freshwater ecosystems. *Can J Fish Aquat Sci* **56**: 1801–1808.

Iversen MH, Ploug H. (2010). Ballast minerals and the sinking carbon flux in the ocean: Carbon-specific

respiration rates and sinking velocity of marine snow aggregates. *Biogeosciences* **7**: 2613–2624.

Iversen MH, Ploug H. (2013). Temperature effects on carbon-specific respiration rate and sinking velocity of diatom aggregates - potential implications for deep ocean export processes. *Biogeosciences* **10**: 4073–4085.

Johnson KS, Riser SC, Karl DM. (2010). Nitrate supply from deep to near-surface waters of the North Pacific subtropical gyre. *Nature* **465**: 1062–1065.

Kabir AH, El-Shehawy R. (2012). Expression of nifH, hetR, and ndaF genes in *Nodularia spumigena* under nitrogen sources. *Plant Biosystems* **146**: 992–1000.

Karl D, Michaels A, Bergman B, Capone D, Carpenter E, Letelier R *et al.* (2002). Dinitrogen fixation in the world's oceans. *Biogeochemistry* **57-58**: 47–98.

Karl DM, Bates NR, Emerson S, Harrison PJ, Jeandel C, Llinas O *et al.* (2003). Temporal studies of biogeochemical processes determined from ocean time-series observations during the JGOFS era. In: Fasham MJR (ed) *Ocean biogeochemistry: the role of the ocean carbon cycle in global change. Global Change—The IGBP Series*. Springer-Verlag: Berlin, pp 239–267.

Kiørboe T, Grossart HP, Ploug H, Tang K. (2002). Mechanisms and rates of bacterial colonization of sinking aggregates. *Appl Environ Microbiol* **68**: 3996–4006.

Kuypers MMM, Lavik G, Woebken D, Schmid M, Fuchs BM, Amann R *et al.* (2005). Massive nitrogen loss from the Benguela upwelling system through anaerobic ammonium oxidation. *Proc Natl Acad Sci USA* **102**: 6478–6483.

Lam P, Kuypers MMM. (2011). Microbial nitrogen cycling processes in oxygen minimum zones. *Ann Rev Mar Sci* **3**: 317–345.

Lavik G, Stührmann T, Brüchert V, Van Der Plas A, Mohrholz V, Lam P *et al.* (2009). Detoxification of sulphidic African shelf waters by blooming chemolithotrophs. *Nature* **457**: 581–584.

Li YH, Gregory S. (1974). Diffusion of ions in sea water and in deep-sea sediments. *Geochim Cosmochim Acta* **38**: 703–714.

Martin JH, Knauer GA, Karl DM, Broenkow WW. (1987). VERTEX: carbon cycling in the northeast Pacific. *Deep Sea Research Part A, Oceanographic Research Papers* **34**: 267–285.

Mohr W, Grosskopf T, Wallace DW, LaRoche J. (2010). Methodological underestimation of oceanic nitrogen fixation rates. *PLoS One* **5**: e12583.

Montoya JP, Voss M, Kähler P, Capone DG. (1996). A simple, high-precision, high-sensitivity tracer assay for N_2 fixation. *Appl Environ Microbiol* **62**: 986–993.

Mulholland MR, Capone DG. (2000). The nitrogen physiology of the marine N_2-fixing cyanobacteria *Trichodosmium* spp. *Trends Plant Sci* **5**: 148–153.

Nielsen LP. (1992). Denitrification in sediment determined from nitrogen isotope pairing. *FEMS Microbiol Ecol* **86**: 357–362.

Paerl HW, Bebout BM. (1988). Direct measurement of O_2-depleted microzones in marine Oscillatoria: Relation to N_2 fixation. *Science* **241**: 442–445.

Paerl HW, Kuparinen J. (2003). Aggregates and Consortia, Microbial. *Encyclopedia of Environmental Microbiology*. John Wiley & Sons, Inc.

Ploug H, Grossart HP, Azam F, Jørgensen BB. (1999). Photosynthesis, respiration, and carbon turnover in sinking marine snow from surface waters of Southern California Bight: Implications for the carbon cycle in the ocean. *Mar Ecol Prog Ser* 179: 1–11.

Ploug H. (2008). Cyanobacterial surface blooms formed by *Aphanizomenon* sp. and *Nodularia spumigena* in the Baltic Sea: Small-scale fluxes, pH, and oxygen microenvironments. *Limnol Oceanogr* **53**: 914–921.

Ploug H, Adam B, Musat N, Kalvelage T, Lavik G, Wolf-Gladrow D *et al.* (2011). Carbon, nitrogen and O_2 fluxes associated with the cyanobacterium *Nodularia spumigena* in the Baltic Sea. *ISME J* **5**: 1549–1558.

Ploug H, Grossart HP. (1999). Bacterial production and respiration in suspended aggregates - A matter of the incubation method. *Aquat Microb Ecol* **20**: 21–29.

Ploug H, Iversen MH, Fischer G. (2008). Ballast, sinking velocity, and apparent diffusivity within marine snow and zooplankton fecal pellets: Implications for substrate turnover by attached bacteria. *Limnol Oceanogr* **53**: 1878–1886.

Ploug H, Jørgensen BB. (1999). A net-jet flow system for mass transfer and microsensor studies of sinking aggregates. *Mar Ecol Prog Ser* **176**: 279–290.

Ploug H, Kühl M, Buchholz-Cleven B, Jørgensen BB. (1997). Anoxic aggregates - An ephemeral phenomenon in the pelagic environment? *Aquat Microb Ecol* **13**: 285–294.

Ploug H, Musat N, Adam B, Moraru CL, Lavik G, Vagner T *et al.* (2010). Carbon and nitrogen fluxes associated with the cyanobacterium *Aphanizomenon* sp. in the Baltic Sea. *ISME J* **4**: 1215–1223.

Ploug H, Zimmermann-Timm H, Schweitzer B. (2002). Microbial communities and respiration on aggregates in the Elbe Estuary, Germany. *Aquat Microb Ecol* **27**: 241–248.

Rahav E, Bar-Zeev E, Ohayon S, Elifantz H, Belkin N, Herut B *et al.* (2013). Dinitrogen fixation in aphotic oxygenated marine environments. *Front Microbiol* **4**: 227.

Revsbech NP. (1989). An oxygen microelectrode with a guard cathode. *Limnol Oceanogr* **34**: 474–478.

Salomon PS, Janson S, Granéli E. (2003). Molecular identification of bacteria associated with filaments of *Nodularia spumigena* and their effect on the cyanobacterial growth. *Harmful Algae* **2**: 261–272.

Simon M, Grossart HP, Schweitzer B, Ploug H. (2002). Microbial ecology of organic aggregates in aquatic ecosystems. *Aquat Microb Ecol* **28**: 175–211.

Stief P, Behrendt A, Lavik G, De Beer D. (2010). Combined gel probe and isotope labeling technique for measuring dissimilatory nitrate reduction to ammonium in sediments at millimeter-level resolution. *Appl Environ Microbiol* **76**: 6239–6247.

Stoecker D, Autio R, Rintala JM, Kuosa H. (2005). Ecto-cellular enzyme activity associated with filamentous cyanobacteria. *Aquat Microb Ecol* **40**: 151–161.

Strous M, Kuenen JG, Jetten MSM. (1999). Key physiology of anaerobic ammonium oxidation. *Appl Environ Microbiol* **65**: 3248–3250.

Takaya N, Catalan-Sakairi MAB, Sakaguchi Y, Kato I, Zhou Z, Shoun H. (2003). Aerobic denitrifying bacteria that produce low levels of nitrous oxide. *Appl Environ Microbiol* **69**: 3152–3157.

Thamdrup B, Dalsgaard T. (2002). Production of N_2 through anaerobic ammonium oxidation coupled to nitrate reduction in marine sediments. *Appl Environ Microbiol* **68**: 1312–1318.

Thomsen JK, Geest T, Cox RP. (1994). Mass spectrometric studies of the effect of pH on the accumulation of

intermediates in denitrification by *Paracoccus denitrificans*. *Appl Environ Microbiol* **60**: 536–541.

Tuomainen J, Hietanen S, Kuparinen J, Martikainen PJ, Servomaa K. (2006). Community structure of the bacteria associated with *Nodularia* sp. (cyanobacteria) aggregates in the Baltic Sea. *Microb Ecol* **52**: 513–522.

Tuomainen JM, Hietanen S, Kuparinen J, Martikainen PJ, Servomaa K. (2003). Baltic Sea cyanobacterial bloom contains denitrification and nitrification genes, but has negligible denitrification activity. *FEMS Microbiol Ecol* **45**: 83–96.

Ulloa O, Canfield DE, DeLong EF, Letelier RM, Stewart FJ. (2012). Microbial oceanography of anoxic oxygen minimum zones. *Proc Natl Acad Sci USA* **109**: 15996–16003.

Van Hulle SWH, Vandeweyer HJP, Meesschaert BD, Vanrolleghem PA, Dejans P, Dumoulin A. (2010). Engineering aspects and practical application of autotrophic nitrogen removal from nitrogen rich streams. *Chem Eng J* **162**: 1–20.

Vintila S, El-Shehawy R. (2010). Variability in the response of the cyanobacterium *Nodularia spumigena* to nitrogen supplementation. *J Environ Monit* **12**: 1885–1890.

Ward BB, Capone DG, Zehr JP. (2007). What's new in the nitrogen cycle? *Oceanography* **20**: 101–109.

Warembourg FR. (1993). Nitrogen fixation in soil and plant system. In: Knowles R, Blackburn TH (eds) *Nitrogen isotopes techniques*. Academic Press: New York, pp 127–155.

Wright JJ, Konwar KM, Hallam SJ. (2012). Microbial ecology of expanding oxygen minimum zones. *Nat Rev Microbiol* **10**: 381–394.

Yoshinari T, Knowles R. (1976). Acetylene inhibition of nitrous oxide reduction by denitrifying bacteria. *Biochem Biophys Res Commun* **69**: 705–710.

Zumft WG. (1997). Cell biology and molecular basis of denitrification. *Microbiol Mol Biol Rev* **61**: 533–616.